Exact, $E = 0$, classical solutions for general power-law potentials

Jamil Daboul*

Physics Department, Ben Gurion University of the Negev, Beer Sheva, Israel

Michael Martin Nieto†

Theoretical Division, Los Alamos National Laboratory, University of California, Los Alamos, New Mexico 87545

For zero energy, $E = 0$, we derive exact, classical solutions for *all* power-law potentials, $V(r) = -\gamma/r^\nu$, with $\gamma > 0$ and $-\infty < \nu < \infty$. When the angular momentum is nonzero, these solutions lead to the orbits $\rho(t) = (\cos\{\mu[\varphi(t) - \varphi_0(t)]\})^{1/\mu}$, for all $\mu \equiv \nu/2 - 1 \neq 0$. When $\nu > 2$, the orbits are bound and go through the origin. This leads to discrete discontinuities in the functional dependence of $\varphi(t)$ and $\varphi_0(t)$, as functions of t, as the orbits pass through the origin. We describe a procedure to connect different analytic solutions for successive orbits at the origin. We calculate the periods and precessions of these bound orbits, and graph a number of specific examples. In addition to the special $\nu = 2$ case, the unbound trajectories are also discussed in detail. This includes the unusual trajectories which have finite travel times to infinity.

PACS number(s): 03.20.+i, 03.65.Sq, 46.10.+z

I. INTRODUCTION

Since the birth of quantum mechanics, studying the connections between classical and quantum physics has been an enormous industry [1–3]. Both the intuitive and the analytic aspects have been studied. In particular, one can observe a kind of "Folk theorem." Problems that are amenable to well-defined, exact, analytic solutions tend to be solvable in both the classical and the quantum regimes.

For example, the fundamental three-dimensional problems of quantum mechanics, the harmonic oscillator and the hydrogen atom, are those classical problems which, by Bertrand's theorem [4], have exact, closed orbits for all energies. The standard, one-dimensional, quantum-mechanical potential problems that are exactly solvable, such as the Morse [5], Rosen-Morse [6], and Pöschl-Teller [7] potentials, are also solvable classically [8–10]. Further, it has even been shown that quantum problems which are solvable, but have certain "mathematical diseases," manifest these diseases already in the classical problem [11].

Usually, when one solves a potential system, one takes a particular potential from a family and solves it for all values of the energy, E. Here, we are going to do the opposite. We will consider the entire class of power-law potentials, parametrized as

$$V(r) = -\frac{\gamma}{r^\nu} = -\frac{\gamma}{r^{2\mu+2}} \ , \qquad \gamma > 0 \ , \qquad -\infty < \nu < \infty \ ,$$

$$(1)$$

and exactly solve it for all ν with the particular energy

*Electronic address: daboul@bguvms.bgu.ac.il
†Electronic address: mmn@pion.lanl.gov

$E = 0$. Note that it will be useful to switch back and forth between the variables ν and μ, related by

$$\mu = (\nu - 2)/2, \qquad \nu = 2(\mu + 1). \qquad (2)$$

The potentials (1) are attractive for $\nu > 0$ and repulsive for $\nu < 0$. For $\nu = 0$, the potential is a constant, $V(r) = -\gamma$, so the particle is force-free.

The above system is exactly solvable in both the classical and quantum-mechanical cases, and there are similarities in the properties of the solutions. In the present paper we shall discuss the very unusual and enlightening classical solutions. Elsewhere [12] we will solve the quantum problem and discuss the wave functions.

The main body of this paper concentrates on the interesting general solutions, with nonzero angular momentum. (In the Appendix we give, for completeness, the simple solutions for zero angular momentum.)

We begin, in Sec. II, by first defining the units which allow us to simplify the equations and their solutions. Then we derive the general $E = 0$ solutions, using two methods. In Sec. III we investigate the general properties of the bound orbits, $\nu > 2$ or $\mu > 0$, such as their precessions and periods.

Continuing, in Sec. IV we graphically depict examples of the bound orbits, thereby demonstrating the general properties derived previously. For $\nu > 4$, the typical solution looks like a flower with several petals. A single orbit describes what we will call a "petal." It starts at the origin, goes out to $r = a$, and returns to the origin. The following orbits then go on to describe further petals which in general are precessed from each other. After a number of petals, the trajectory closes if ν is a rational fraction. The petals are very thin for large ν, but become wider and wider as ν decreases from infinity. When $\nu = 4$ the orbit does not precess. It describes a circle which goes through the origin and continually repeats itself.

For $4 > \nu > 2$, the orbits become tighter and tighter spirals in and out of the origin as $\nu \to 2$. Once again, for ν being a rational fraction, the orbits eventually close on themselves.

It is to be emphasized that the joining of the successive orbits at the origin, as described above, demands special attention. This is because the potential is singular at the origin. Conservation of linear and angular momentum is used to impose physical boundary conditions.

In Sec. V we discuss the special $\nu = 2$ case, which is a boundary case between bound and unbound trajectories. The classically unbound trajectories, given by $\nu < 2$, are covered in Sec. VI. We close with a discussion, and defer comparisons between the classical and quantum problems to Ref. [12].

II. GENERAL SOLUTIONS

A. Classical turning point as a unit of length

Power-law potentials do not have a built-in length scale. Therefore, it is convenient in our $E = 0$ case to define a length scale, a, to be the radius of the turning point. This is the radius at which the effective potential vanishes:

$$U(L, r) = \frac{L^2}{2mr^2} - \frac{\gamma}{r^\nu} \tag{3}$$

$$= \frac{L^2}{2ma^2} \left(\frac{1}{\rho^2} - \frac{1}{\rho^\nu} \right) , \qquad \rho = \frac{r}{a} , \tag{4}$$

where a is determined by the condition $U(L, a) = 0$:

$$a = \left(\frac{2m\gamma}{L^2} \right)^{\frac{1}{2\mu}} = \left(\frac{2m\gamma}{L^2} \right)^{\frac{1}{\nu-2}} , \qquad \nu \neq 2 , \quad \mu \neq 0 . \tag{5}$$

Note that in these units, V is given by

$$V(r) = -\frac{\gamma}{r^\nu} = -\frac{L^2}{2ma^2} \frac{1}{\rho^\nu} = -\frac{L^2 a^{\nu-2}}{2m} \frac{1}{r^\nu} . \tag{6}$$

B. From the orbit equation

A direct, mathematically inspired solution can be obtained by integrating the orbit equation [13, 14]

$$\varphi - \varphi_0 = \int_{r_0}^{r} \frac{r^{-1} \, dr}{\sqrt{\frac{2m}{L^2}(E - V)r^2 - 1}} . \tag{7}$$

The general solution has the constant φ_0 in it. We presciently set $\varphi_0 = 0$ when $\rho = 1$ (the turning-point condition), so that the turning point is along the positive x axis.

Then, setting $E = 0$ makes the integral (7) doable for all ν. Changing variables successively to $\rho = r/a$, $y = \rho^\mu$, and $x = \cos^{-1} y$ means that Eq. (7) can be written as

$$\varphi = \int_{1}^{\rho} \frac{\rho^{(\mu-1)} \, d\rho}{\sqrt{1 - \rho^{2\mu}}} = \mu^{-1} \int_{1}^{y} \frac{dy}{\sqrt{1 - y^2}}$$

$$= -\mu^{-1} \int_{0}^{\cos^{-1} y} dx . \tag{8}$$

Therefore, the solution is

$$\rho^\mu = y = \cos(-\mu\varphi) = \cos(\mu\varphi) , \tag{9}$$

or

$$\rho = \left[\cos \left(\frac{(\nu - 2)\varphi}{2} \right) \right]^{\frac{2}{\nu-2}} = [\cos(\mu\varphi)]^{1/\mu} . \tag{10}$$

We will discuss the allowed angular variations of φ in the separate sections on bound and unbound orbits.

C. From the energy-conservation equation

We now give a more intuitive derivation of the solution (10). By substituting the angular-momentum conservation condition

$$\dot{\varphi} = L/(mr^2) \tag{11}$$

into the energy-conservation condition

$$E = T + V = \frac{m}{2} \dot{\varphi}^2 \left[\left(\frac{dr}{d\varphi} \right)^2 + r^2 \right] + V , \tag{12}$$

one obtains [15, 16]

$$\left(\frac{dr}{d\varphi} \right)^2 + r^2 = \frac{2m(E - V)r^4}{L^2} . \tag{13}$$

This is essentially a first-order differential equation, which can be formally integrated to yield the angular equation (7) of the last subsection.

However, for $E = 0$, it is much more efficient to solve Eq. (13) directly. Converting to the dimensionless variable $\rho = r/a$ and substituting V from Eq. (6) into Eq. (13), we obtain

$$\left(\frac{d\rho}{d\varphi} \right)^2 + \rho^2 = \rho^{(4-\nu)} = \rho^{(2-2\mu)}. \tag{14}$$

For $\nu = 4$ the right-hand side of this equation is unity, so the solution is a cosine. This is the circular orbit $\rho = \cos \varphi$ which we will discuss in detail in the next section. Guided by this and the substitution $y = \rho^\mu$ of the last subsection, we multiply Eq. (14) by $\rho^{2\mu-2}$ to yield

$$\left(\rho^{\mu-1} \frac{d\rho}{d\varphi} \right)^2 + \rho^{2\mu} = \left(\frac{d\rho^\mu}{\mu d\varphi} \right)^2 + (\rho^\mu)^2 = 1 . \tag{15}$$

Now ρ^μ satisfies the differential equation for the trigonometric functions. Therefore, the *general* solution of Eq. (15) is given by

$$\rho^\mu = \cos\{ \mu(\varphi - \varphi_0) \} = \cos \left[\frac{\nu - 2}{2} (\varphi - \varphi_0) \right] , \tag{16}$$

or

$$\rho = \cos\{\mu\left[(\varphi - \varphi_0)\right]\}^{1/\mu}$$

$$= \left[\cos\left(\frac{\nu - 2}{2}(\varphi - \varphi_0)\right)\right]^{\frac{2}{\nu - 2}} . \qquad (17)$$

The phase, φ_0, is the integration constant. It depends on the initial conditions and, as before, we will set φ_0 to zero for our first-orbit turning-point condition.

III. PROPERTIES OF THE BOUND TRAJECTORIES: $2 < \nu$ OR $1 < \mu$

In Fig. 1 we show a typical effective potential $U(r)$ in this regime. One sees that the value of $U(r)$ starts from $-\infty$ at $r = 0$, rises through zero at $r = a$, reaches a maximum, and then decreases to zero at $r \to \infty$. Therefore, the $E = 0$ solution for $r = r(t)$ can only vary between $r = 0$ and $r = a$. We shall now discuss the dependence of r on the azimuthal angle, φ.

A. The first orbit

The radius, ρ, is non-negative. This means the range of the angle variable for the first orbit is restricted. Since, by convention, the first orbit has $\varphi_0 = \varphi_0^1 = 0$, this means $\varphi^1 = \varphi$ satisfies

$$-\frac{\pi}{2\mu} = -\frac{\pi}{\nu - 2} \le \varphi^1 \le \frac{\pi}{\nu - 2} = \frac{\pi}{2\mu} . \qquad (18)$$

The corresponding curve $\rho = \rho(\varphi^1)$ in the x-y plane begins at $\rho = 0$ for $\varphi^1 = -\pi/2\mu = -\pi/(\nu - 2)$, evolves counterclockwise to $\rho = 1$ at $\varphi^1 = 0$, and then continues on back to $\rho = 0$ at $\varphi^1 = \pi/(2\mu) = \pi/(\nu - 2)$. The curve evolves counterclockwise because we have chosen, by convention, that the angular momentum is in the positive z direction. (Of course, there is also a mathematically rotated clockwise solution.)

Every such closed circuit, beginning and ending at the origin, we will call an *orbit*. Because of the shapes of the orbits (which we will present in the next section), when $\nu > 4$ we will also call an orbit a *petal* (of a flower) and when $\nu < 4$ we will also call an orbit a *spiral*, which
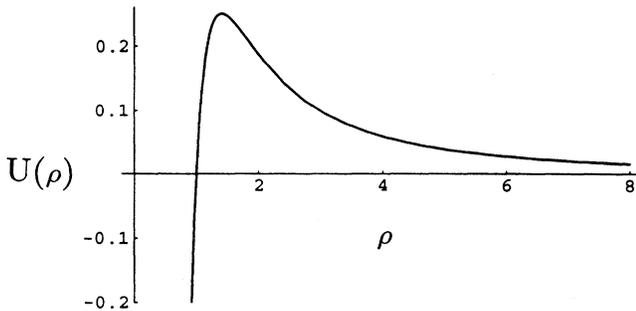
actually is a double spiral since it spirals out and then spirals in. These two classes of orbits meet at $\nu = 4$, which is the circle that goes through the origin. As we will see below, the entire physical trajectory will consist of a pattern of either (i) a finite integral number of orbits which then repeat over themselves, when μ is a rational number, or else (ii) an infinite number of nonrepeating orbits, if μ is an irrational number. (In Sec. VI we will discuss the classically unbound orbits described by $\nu \le 2$ or $\mu \le 1$.)

B. Solutions for later bound orbits

1. The angles and the phase shifts

To obtain the entire physical solution, we must connect different orbits. That is, the first orbit evolves into the second orbit...evolves into the kth orbit. Because the orbits go through the origin, both φ and φ_0 are discontinuous, as we will demonstrate below. Therefore, we will label φ and φ_0 for the kth orbit as φ^k and φ_0^k, respectively.

The successive orbits must be connected at the origin, $r = 0$. How this is done is a choice of boundary conditions at the singularity and affects the resultant physics. (This is similar to how the quantum choice of boundary condions will lead to different self-adjoint extensions of the Hamiltonian. See Ref. [12].) One could, for example, take the conditions to be a hard core reflection.

However, we choose as the appropriate physics that the directions of the linear momentum $\hat{\mathbf{p}}$ and the angular momentum $\mathbf{L}$ are continuous functions of time. We *defined* the first orbit to have its apogee, $r = a$, at $\varphi^1 = 0$, which corresponded to the choice $\varphi_0^1 = 0$. In order to obtain this physical solution, we must connect the first orbit to the second orbit in such a way that the tangent vector to the combined trajectory is continuous at the origin.

Before the particle starts the second orbit, the trajectory goes though the origin. This creates a singular transition in the polar coordinates. (Since the trajectory passes through the origin and because $\hat{\mathbf{p}}$ must be continuous, the direction $\hat{\mathbf{r}}$ of the position vector must change sign at $r = 0$.) The angle advances by π (instead of $-\pi$) in going through the origin because, in order to conserve angular momentum, the position vector must continue rotating in the counterclockwise direction. Then the particle begins its second orbit, traveling another angular distance π/μ. Before beginning its third orbit, the particle goes through the origin again, advancing another π radians. Therefore, the angular variation of the kth orbit, φ^k, is given by

$$\varphi_{\min}^k \equiv \left(\frac{(k - 3/2)}{\mu} + (k - 1)\right)\pi \le \varphi^k$$

$$\le \left(\frac{(k - 1/2)}{\mu} + (k - 1)\right)\pi \equiv \varphi_{\max}^k \qquad (19)$$

and one has the condition

$$\varphi_{\min}^{k+1} = \varphi_{\max}^k + \pi . \qquad (20)$$

FIG. 1. For $\nu = 4$ a plot of the effective potential, U, as a function of ρ. [See Eq. (3).] $U(\rho) = [1/\rho^2 - 1/\rho^4]$.

However, the phase shift, φ_0^k, must also change with each orbit. Recall, in summary, that the kth orbit is described in polar coordinates by

$$\rho_k = [\cos\{\mu(\varphi^k - \varphi_0^k)\}]^{1/\mu} , \qquad (21)$$

with

$$|\varphi^k - \varphi_0^k| \leq \pi/2\mu \qquad (22)$$

or, equivalently,

$$\varphi_{\min}^k \equiv \varphi_0^k - \frac{\pi}{2\mu} \leq \varphi^k \leq \varphi_0^k + \frac{\pi}{2\mu} \equiv \varphi_{\max}^k . \qquad (23)$$

Then, from Eqs. (19) and (23), the phase shift, φ_0^k, is

$$\varphi_0^k = \frac{\varphi_{\min}^k + \varphi_{\max}^k}{2}$$
$$= (k-1)\left(\frac{\nu}{\nu - 2}\right)\pi$$
$$= (k-1)\left(1 + \frac{1}{\mu}\right)\pi . \qquad (24)$$

Mathematically this change of phase shift, φ_0^k, with each orbit is because the orbit must be symmetric about any apsidal vector [17]. This is true even though the vector is zero length from the origin. (See the interesting application of these concepts in the $\nu = 6$ orbit discussion of the next section.) Further, the other apsidal vectors, $\mathbf{r}_k(\varphi^k = \varphi_0^k)$, are the symmetry axes of the kth orbits.

2. Angle vs phase-shift differences

It is instructive to observe that, instead of using the label, k, for each orbit, formally we can write the general solution for all times $t \geq 0$ in the form

$$\rho(t) = (\cos\{\mu[\varphi(t) - \varphi_0(t)]\})^{1/\mu} \equiv [\cos\mu\chi(t)]^{1/\mu} , \qquad (25)$$

with

$$\chi(t) \equiv \varphi(t) - \varphi_0(t) . \qquad (26)$$

Here, both the azimuthal angle, φ, and also the phase shift, φ_0, are regarded as functions of time. These angles have discrete jumps at the crossing times

$$t_k \equiv (k - 1/2)\tau , \qquad (27)$$

where the t_k are the times at which the particle passes through the origin and τ is the period of one orbit. Using our same physical convention, which here is $r(0) = a$ at $t = 0$ with $\varphi(0) = \varphi_0(0) = 0$, we have that the jumps are

$$\varphi(t_k + \epsilon) = \varphi(t_k - \epsilon) + \pi \qquad (28)$$

and

$$\varphi_0(t) = \pi\left(1 + \frac{1}{\mu}\right)\sum_{k=1}^{\infty}\Theta(t - t_k) , \qquad (29)$$

where $\Theta(t)$ is the Heaviside step function.

We see that both φ and φ_0 are monotonically increas-

ing functions of time. In contrast, their difference, $\chi(t)$, is a periodic function of t. For every new orbit, χ starts with the value $-\pi/(2\mu)$ and then increases monotonically to $\pi/(2\mu)$, due to the continuous increase in $\varphi(t)$ as the particle goes through one orbit (petal or spiral). Next, χ decreases stepwise by π/μ at the crossing time. Therefore, as in our previous representation, $\cos\mu\chi$ starts and ends each orbit at $\rho = 0$.

C. Precession of the orbits

Because of angular-momentum conservation, the azimuthal angle, φ, is a monotonic function of time, t. If there is no precession, φ *increases* exactly by 2π after one period, τ. However, if after one period the axis of the orbit has rotated *forwards or backwards* (i.e., clockwise or counterclockwise) from 2π by an angle P_ν, then this is the precession per period. Specifically,

$$\varphi(t + \tau) - \varphi(t) = 2\pi + P_\nu , \qquad (30)$$

where τ is the period of one orbit. If we choose t to be the time at which the particle was at the apogee of the kth orbit, then $t + \tau$ will be the time at which the particle reaches the apogee of the $(k + 1)$th orbit. To do this, the particle must first rotate by $\pi/2\mu$ to reach the origin, have its angle φ jump by π at the origin, and finally rotate by another $\pi/2\mu$ to reach the new apogee. Thus, from Eq. (30) we have

$$\varphi(t+\tau)-\varphi(t) = \frac{\pi}{2\mu}+\pi+\frac{\pi}{2\mu} = \left(\frac{1}{\mu}+1\right)\pi = 2\pi+P_\nu , \qquad (31)$$

so that

$$P_\nu = \left(\frac{1}{\mu} - 1\right)\pi = \left(\frac{4 - \nu}{\nu - 2}\right)\pi . \qquad (32)$$

In Fig. 2 we plot P_ν as a function of ν. The precession is infinite at $\nu = 2$, decreases through zero at $\nu = 4$, and asymptotes to $-\pi$ as ν goes to infinity. Therefore, the precession will be zero for $\nu = 4$, negative (counterclockwise) for $\nu > 4$, and positive (clockwise) for $\nu < 4$.

This also demonstrates that, for ν equal to a rational fraction, the orbits will eventually close on themselves, and repeat. This happens when kP_ν is an integer times 2π.

D. Classical period

The classical period, τ, can be obtained by integrating the angular-velocity equation

$$\frac{d\varphi}{dt} = \frac{L}{mr^2} = \frac{1}{\tau_0\rho^2} , \qquad (33)$$

where τ_0 is a convenient unit of time,

$$\tau_0 = \frac{ma^2}{L} . \qquad (34)$$

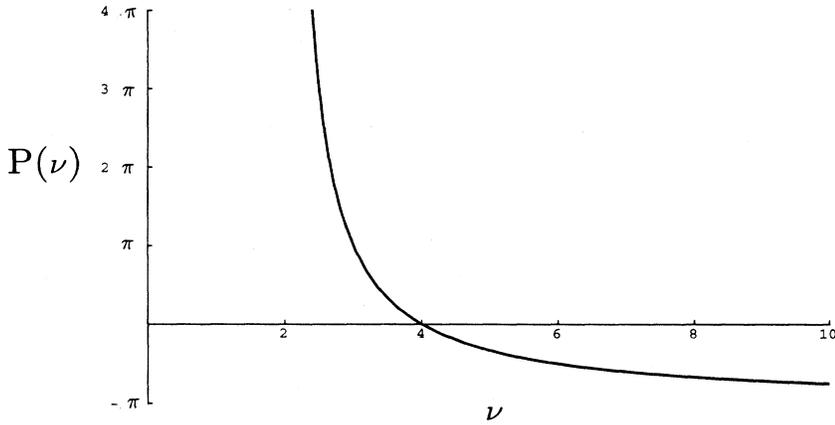One then has that the classical period in units of τ_0 is

FIG. 2. A plot of P_ν, the precession per orbit, as a function of ν.

$$T_\nu = \frac{\tau_\nu}{\tau_0} = \int_{\frac{-\pi}{|\nu-2|}}^{\frac{\pi}{|\nu-2|}} \rho^2(\varphi) \, d\varphi$$

$$= \int_{\frac{-\pi}{2|\mu|}}^{\frac{\pi}{2|\mu|}} [\cos(|\mu|\varphi)]^{\left(\frac{2}{\mu}\right)} \, d\varphi \ . \tag{35}$$

[In Eq. (35) we have inserted absolute values around μ in the arguments of the integral and integrand. This allows us to include the negative μ case that we will return to at the end of this discussion.]

Changing variables to $x = |\mu|\varphi$ allows the integral to be evaluated as [18]

$$T_\nu = \frac{2}{|\mu|} \int_0^{\frac{\pi}{2}} [\cos x]^{\left(\frac{2}{\mu}\right)} \, dx = \frac{1}{|\mu|} B(1/2, \ b) \tag{36}$$

$$= \frac{\sqrt{\pi}}{|\mu|} \frac{\Gamma(b)}{\Gamma(b+1/2)} \ , \qquad b > 0 \ , \tag{37}$$

where

$$b \equiv \frac{1}{\mu} + \frac{1}{2} = \frac{\nu+2}{2\nu-4} > 0 \ . \tag{38}$$

$B(b, c) = \Gamma(b)\Gamma(c)/\Gamma(b + c)$ is the beta function and we used $\Gamma(1/2) = \sqrt{\pi}$. We see that T_ν is finite and well defined for $\mu > 0$ or $\nu > 2$, as would be expected for bound orbits.

In Fig. 3 we plot T_ν as a decreasing function of ν. From Eq. (37) special cases are

$$\lim_{\epsilon \to 0} T_{2+\epsilon} = \left(\frac{2\pi}{\epsilon}\right)^{1/2} , \tag{39}$$

$$T_3 = \frac{3\pi}{4} \ ,$$

$$T_4 = \frac{\pi}{2} \ ,$$

$$T_6 = 1 \ ,$$

$$\lim_{\nu \to \infty} T_\nu = \frac{2\pi}{\nu} \ .$$

The first equality in Eq. (39) is obtained by using [19] the relation $\Gamma(z + 1/2) \simeq \Gamma(z)\sqrt{z}$, which holds for $|z| \to \infty$.

In passing, note that Eqs. (37) and (38) also tell us that T_ν is finite and well defined for the unbound, infinite orbits corresponding to $\mu < -2$ or $\nu < -2$. This means that it takes a finite time for the particle to travel in from
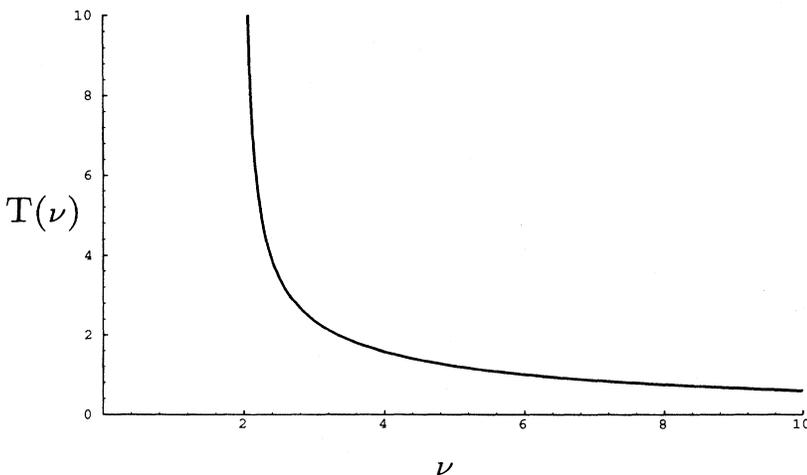

FIG. 3. A plot of the dimensionless orbital period $T_\nu = \tau_\nu/\tau_0$ as a function of ν.

infinity, reach the turning point $r = a$, and then go back to infinity.

IV. EXAMPLES OF CLASSICAL BOUND TRAJECTORIES

A. Petals: $\nu > 4$ or $\mu > 1$

From the preceding section we see that, as ν approaches infinity, the orbit is an ever-narrowing petal of width

$$\Phi_\nu = \frac{\pi}{\mu} = \frac{2\pi}{\nu - 2} . \tag{40}$$

Similarly, the counterclockwise precession reaches $-\pi$ per orbit as $\nu \to \infty$. As ν becomes smaller, the petals increase in width. We illustrate this with several illuminating examples.

$\nu = 8$, *three petals*. We begin with the case $\nu = 8$. Here a petal is $\pi/3$ wide and the precession per orbit is $-2\pi/3$. Thus, there are three orbits before the trajectory closes. Note that the three petals in a closed trajectory cover only half of the opening angle from the origin. We show this in Fig. 4.

$\nu = 7$, *ten petals*. For $\nu = 7$ a petal is $2\pi/5$ wide and the precession per orbit is $-3\pi/5$. This means that, before the trajectory closes, there must be ten orbits and the precession goes around three times.

$\nu = 6$, *perpendicular lemniscates*. The case $\nu = 6$ is very interesting. The width of a petal is $\pi/2$ and the precession is $-\pi/2$ per orbit. Here, the width of a petal

FIG. 5. The first four orbits for $\nu = 6$ or $\mu = 2$. Each orbit is precessed $-\pi/2$ from the previous one, so that by the end of the fourth orbit, the trajectory closes.

and the precession are exactly such that there is no overlap and also no "empty angles." It takes four orbits to close a trajectory. This is shown in Fig. 5. We see that the physical solution consists of two perpendicular lemniscates (figure-eight curves composed of two opposite petals). This conclusion is in contradiction to one given in the literature [20]. There, a single lemniscate was predicted. From the physical arguments we have given
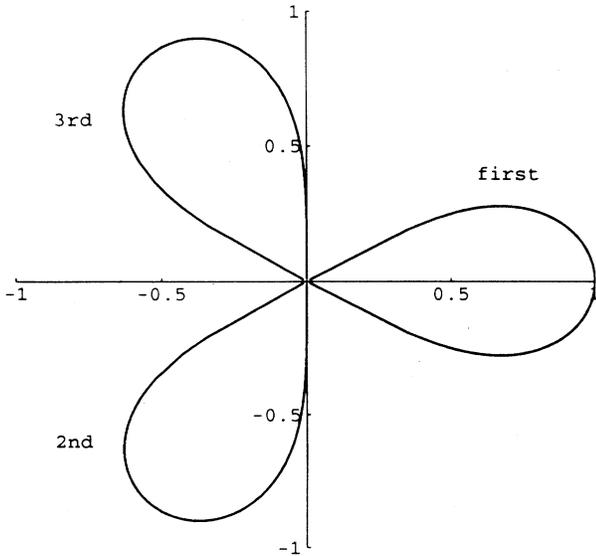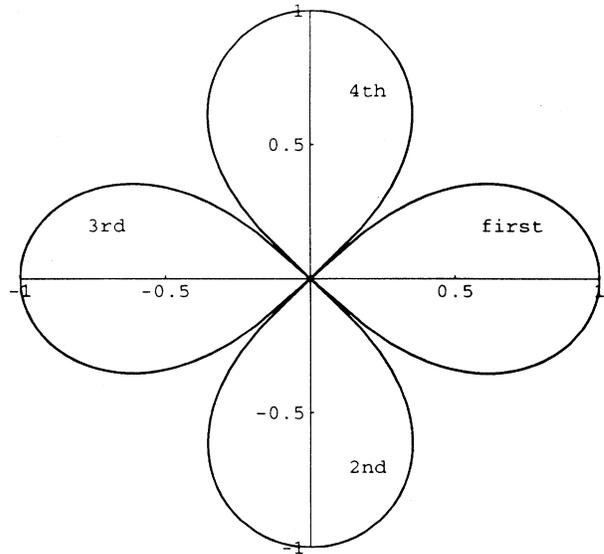

FIG. 4. The first three orbits for $\nu = 8$ or $\mu = 3$. Each orbit is precessed $-2\pi/3$ from the previous one, so that by the end of the third orbit, the trajectory closes. In this and later figures, the radius is in the dimensionless units of ρ. For orientation, we show the dimensionless Cartesian coordinates.
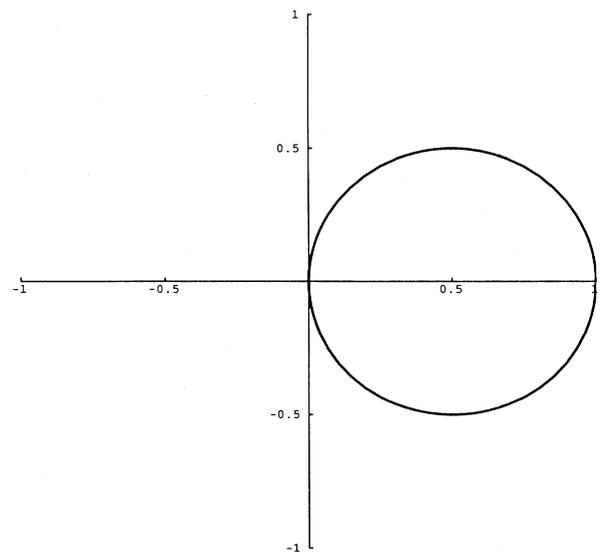

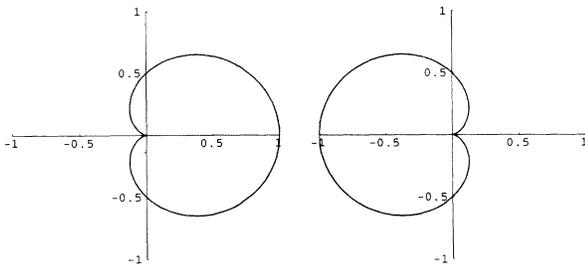FIG. 6. The orbit for $\nu = 4$ or $\mu = 1$. It is a circle, and repeats itself continually.

FIG. 7. The first two orbits for $\nu = 3$ or $\mu = 1/2$. Each orbit is precessed π from the previous one, so that by the end of the second orbit, the trajectory closes.

FIG. 9. Close-up details of the beginning of the first orbit for $\nu = 7/3$ or $\mu = 1/6$. The orbit starts at $\varphi = -3\pi$. The four graphs show the evolution for (a) $-3\pi \le \varphi \le -2.91\pi$, (b) $-3\pi \le \varphi \le -5\pi/2$, (c) $-3\pi \le \varphi \le -2\pi$, and (d) $-3\pi \le \varphi \le -\pi$.

above, this is not valid. This incorrect solution resulted from studying the equation for the square of the orbit.

$\nu = 5$, *six overlapping petals*. The petals are $2\pi/3$ wide and they precess by $-\pi/3$ per orbit. This means there are six petals in a closed trajectory (flower). Note that here a petal is still so wide and the precession is so small that the successive petals overlap.

B. Circle through the origin: $\nu = 4$ or $\mu = 1$

For $\nu = 4$, the solution is well known [21]. It is a circle that starts at the origin, travels symmetrically about the positive x axis, and returns to the origin. The precession is zero, so the orbit continually repeats itself. In Fig. 6 we show the orbit.

C. Double spirals: $2 < \nu < 4$ or $0 < \mu < 1$

As ν becomes less than 4, we can think of a petal obtaining a width greater than π, i.e., an orbit consists of two spirals, one out and one in, at opposite ends of the orbit. As ν approaches 2, the spirals become tighter and tighter and the precession (now clockwise) becomes larger. In fact, the spirals' angular variation as well as the orbit's precession both become infinite in magnitude
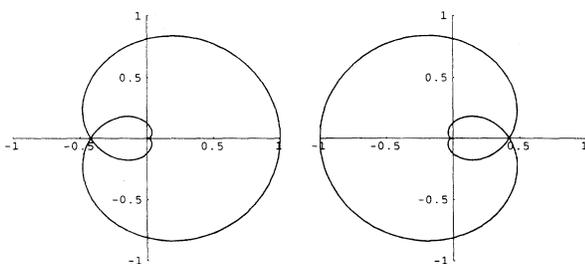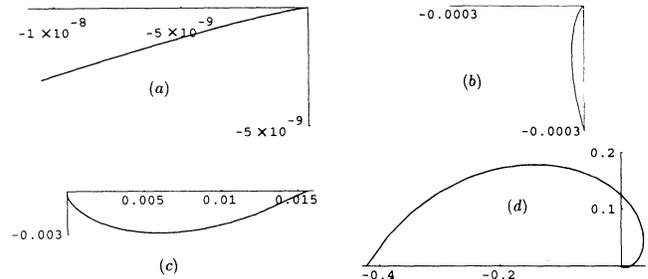

FIG. 8. The first two orbits for $\nu = 7/3$ or $\mu = 1/6$. Each orbit is precessed 5π from the previous one, so that by the end of the second orbit, the trajectory closes.

as ν approaches 2.

Consider the special case $\nu = 3$. The width of the double-spiral orbit is still given by the formula for Φ_ν, and is 2π. Therefore, the first orbit begins and ends towards the negative x axis. The precession is π, so the trajectory closes after two orbits. We show this case in Fig. 7.

When $\nu = 7/3$, the width of the double spiral is 6π. This means the first orbit starts towards the negative x axis, winds around one and a half times before reaching the positive axis, and then winds one and a half times more to reach the origin again. The precession is 5π, so the trajectory closes after two orbits. We show this case in Fig. 8. However, on this scale it is impossible to see the tight winding of the spirals near the origin. Therefore, we demonstrate it with expanded views in Fig. 9.

As $\nu \to 2$ from above, the spirals get tighter and tighter. Their angular widths, $\Phi_\nu = 2\pi/|\nu - 2|$, become larger and larger as $\nu \to 2$.

V. THE BOUNDARY BETWEEN UNBOUND AND BOUND CLASSICAL TRAJECTORIES: $\nu = 2$ OR $\mu = 0$

For $\nu = 2$ or $\mu = 0$, there is no natural length scale. Both the external and the centripetal potentials have the same power dependence on r, so that the effective potential of Eq. (3) is

$$U(r) = (L^2/2m - \gamma)\frac{1}{r^2} \ . \tag{41}$$

We have three distinct physical situations depending on whether $L^2/2m > \gamma$, $L^2/2m = \gamma$, or $L^2/2m < \gamma$. Then for all r the effective potential $U(r)$ is either repulsive (and positive-valued), identically zero, or attractive (and negative-valued).

For $U(r) > 0$ there is no solution for $E = 0$. For $U(r) \equiv 0$ the orbit is a circle, which we discuss in the next subsection. Finally, for $U(r) < 0$, the solution is an infinite spiral described in Sec. V B.

A. The circular bound orbit: $r = a$

For $U(\rho) \equiv 0$, Eq. (14) yields $d\rho/d\varphi = 0$. The solution is a circle, $r = a$ or $\rho = r/a = 1$, whose radius is determined by the initial conditions.

This particular solution also follows from our general solution (10) by taking the $\mu \to 0$ limit. The value of the limit, which is

$$\lim_{\mu \to 0} (\cos \mu\varphi)^{\frac{1}{\mu}} = 1 \; , \tag{42}$$

can be obtained from

$$\lim_{\mu \to 0} \ln(\cos \mu\varphi)^{\frac{1}{\mu}} = \lim_{\mu \to 0} \frac{\ln(\cos \mu\varphi)}{\mu}$$
$$= \lim_{\mu \to 0} \frac{1}{\mu}(-\mu^2\varphi^2/2 + \cdots) \to 0 \; . \tag{43}$$

Physically we know that this orbit has a finite period, since the period is the time it takes the particle to rotate from $\varphi = 0$ back to the same physical point when $\varphi = 2\pi$. Even so, the formula for T_ν yields infinity in the limit $\mu \to 0$. The reason is that as $\nu \to 2$ from above, the orbit is a double spiral that winds more and more times: i.e., $\Phi_\nu \to \infty$. The windings get closer and closer to the circle $\rho = 1$. In effect, $\nu = 2$ can be considered as the limit when the infinite number of windings all overlap the circle.

B. The unbound infinite spiral

For $U(r) < 0$ the result cannot be regarded as a special case of the general solution (17). This is not unexpected since the general solution satisfies the initial conditions $r(0) = a$ and $dr(0)/d\varphi = 0$. This means $r = a$ is a turning point. However, for $U(r) < 0$ these conditions can never be satisfied. [See Eq. (45) below.] Nevertheless, there is a different and interesting $E = 0$ solution, as we now show.

Since $U < 0$, the energy-conservation condition (12) for $E = 0$ gives

$$\left(\frac{dr}{d\varphi}\right)^2 = \left(2m\gamma/L^2 - 1\right) r^2 \equiv \lambda^2 r^2 \; , \tag{44}$$

so that

$$dr/d\varphi = \mp\lambda r \; . \tag{45}$$

Therefore, the two possible solutions are

$$r = r_0 \exp\left[\mp\lambda \left(\varphi - \varphi_0\right)\right] \; , \qquad -\infty < \varphi < \infty \; . \tag{46}$$

These correspond to orbits which pass through the point (r_0, φ_0) and spiral inwards or outwards for the minus or plus signs, respectively. For example, a complete, counterclockwise orbit, starting from the initial value $r = r_{\text{in}} = r(\varphi_{\text{in}})$, going into the origin, and then going out of the origin towards the final value $r = r_f = r(\varphi_f)$, is given by

$$\frac{r}{r_{\text{in}}} = \exp\left[-\lambda \left(\varphi - \varphi_{\text{in}}\right)\right] \; , \qquad \varphi_{\text{in}} \le \varphi < \infty \; , \tag{47}$$

$$\frac{r}{r_f} = \exp\left[+\lambda \left(\varphi - \varphi_f\right)\right] \; , \qquad -\infty < \varphi \le \varphi_f \; . \tag{48}$$

However, it is important to note that Eqs. (47) and (48) are only special cases of Eq. (46). For example, Eq. (46), with the plus sign, can also describe an r starting at $r(\varphi_0) = r_0$ which then goes out to infinity as $\varphi \to \infty$.

Despite the infinite spirals in the example of Eqs. (47) and (48), the journey in and out takes only a finite time. To see this, consider the time dependence of r. From the energy-conservation conditions (12) and (44), we have

$$\dot{r}^2 = \frac{2}{m}\frac{\gamma}{r^2} - \frac{L^2}{m^2r^2} = \frac{L^2}{m^2}\left(\frac{2m\gamma}{L^2} - 1\right)\frac{1}{r^2} = \left(\frac{L\lambda}{m}\right)^2 \frac{1}{r^2} \; . \tag{49}$$

Therefore,

$$\frac{dr^2}{dt} = 2r\dot{r} = \mp\frac{2L\lambda}{m} \tag{50}$$

and

$$r^2 = r_0^2 \mp \frac{2L\lambda}{m}(t - t_0) \; . \tag{51}$$

This tells us that, in spite of the infinite spiraling, a particle moving *inwards* reaches the origin, $r = 0$, from any point r_0 in a finite time, given by

$$\Delta t = t - t_0 = \frac{m}{2L\lambda} r_0^2 \; . \tag{52}$$

Finally, substituting Eq. (46) into Eq. (51) gives the general time dependence of φ as

$$t - t_0 = \mp\frac{m}{2L\lambda}(r^2 - r_0^2) = \mp\frac{mr_0^2}{2L\lambda}\{\exp[\mp2\lambda(\varphi - \varphi_0)] - 1\} \; . \tag{53}$$

Because of our choice $\hat{\mathbf{L}} = \hat{\mathbf{z}}$, in Eq. (53) we are assuming that φ increases monotonically with time.

(The $\nu = 2$ case is special in another way. For $\nu \equiv 2$ and $E \ne 0$, it is the demarcation between the $E < 0$ bound solutions and $E > 0$ unbound solutions. These latter are Cotes' spirals [22]. The $E \ne 0$ solutions are given in Refs. [23, 24].)

VI. UNBOUND TRAJECTORIES: $\nu < 2$ OR $\mu < 0$

A. Properties of unbound trajectories

When the potential parameter ν becomes smaller than 2, that is, when $\nu < 2$ or $\mu < 0$, there is another change. It is as if the "infinite overlapping circle" solution for $\nu = 2$ breaks, and the two ends spiral out to infinity from the point $\rho = 1$ and $\varphi = 0$.

As the value of ν decreases, the value of the angular width of the trajectory, now given by $\Phi_\nu = \pi/|\mu|$, also decreases accordingly. By the time $\nu = 1$, the angular width has decreased to 2π. Eventually it becomes less than π, meaning the orbit comes in and out in the same half-plane. That is, when $\nu < 0$, the force is repulsive. In the next section we give some illustrative examples.
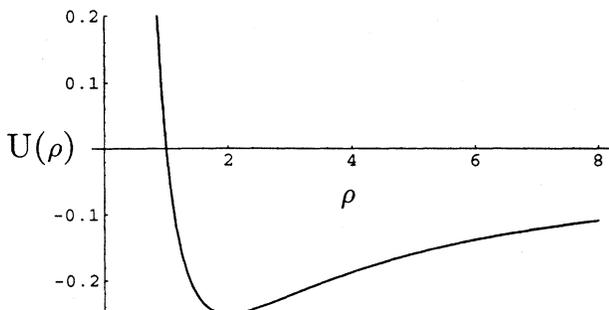
FIG. 10. The effective potential, $U(\rho) = 1/\rho^2 - 1/\rho$, as a function of ρ.

B. Kepler-like potentials: $0 < \nu < 2$ or $-1 < \mu < 0$

When $0 < \nu < 2$, the repulsive centripetal barrier dominates at small r whereas the attractive potential $V = -\gamma/r^\nu$ dominates at large r. A typical shape of the effective potential is sketched in Fig. 10. It is familiar from the Kepler problem. Therefore, for $0 < \nu < 2$, the $E = 0$ classical orbits are all unbounded. The distance, a, defined in Eq. (5) now has a completely different interpretation. It is now the distance of closest approach. Even so, the formal solution (16) remains valid for negative values of μ.

As a first example consider the case $\nu = 3/2$ or $\mu = -1/4$. This orbit has a total angular width of 4π. It is shown in the two drawings of Fig. 11. The large-scale first drawing shows the trajectory coming in from the top, performing some gyration, and going out at the bottom. The small-scale second drawing shows the trajectory winding around twice near the origin, with the distance of closest approach being one.

A second example is the exact Kepler potential, $\nu = 1$ or $\mu = -1/2$. Equation (16) gives

$$\rho^{-1/2} = \cos\varphi/2 , \tag{54}$$

so that

$$\frac{1}{\rho} = (\cos\varphi/2)^2 = \frac{1 + \cos\varphi}{2} . \tag{55}$$

This is the famous parabolic orbit for the Kepler problem with $E = 0$. This orbit is shown in the first drawing of Fig. 12. The parabola yields an angular width of 2π, as it should.

C. The straight line: $\nu = 0$ or $\mu = -1$

If we formally set $\nu = 0$ in expression (1), we get a negative constant potential $V(r) = -\gamma$. Therefore, in this case the force vanishes and we have a free particle. Its orbit must be a straight line,

$$\rho = [\cos\varphi]^{-1} , \qquad x = r\cos\varphi = a . \tag{56}$$

This is the equation for a vertical straight line that crosses the x axis at $x = a$, as required by the initial conditions. This orbit is shown in the second drawing in Fig. 12; it subtends an angular width of π from the origin.

D. Repulsive potentials: $-\infty < \nu < 0$ or $-\infty < \mu < -1$

For $\nu < 0$ the potentials $V(r)$ in Eq. (1) are repulsive and negative-valued for all $r > 0$, with $V(r)$ going to $-\infty$ at large distances. Since both the potential, $V(r)$, and the centripetal potential decrease monotonically, the effective potential has no minima or maxima. Even so, for $E = 0$ these unbounded orbits behave qualitatively like those for $0 \leq \nu < 2$. The distance of closest approach again obeys the formula (5) and the solutions are given by the same expression (16), which is valid for all $\mu \neq 0$.

The solution (16) for the first orbit ($\varphi_0^1 = 0$) gives

$$\rho = [\cos\mu\varphi]^{1/\mu} = [\cos|\mu|\varphi]^{-1/|\mu|} . \tag{57}$$

This shows that the particle is at $r = a$ when $\varphi = 0$ and it is at infinity when $\varphi = \pm\pi/(2|\mu|)$. Thus, these orbits become narrower as $|\mu|$ becomes larger. This is similar to the case of the width of the petals of the bound orbits.

Hyperbolic orbits. The most famous special case of these potentials is the "inverted" harmonic-oscillator po-
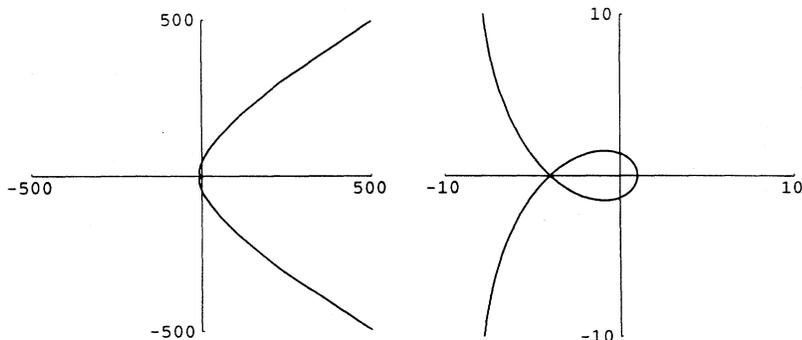

FIG. 11. A large-scale view, and a small-scale view near the origin, of the trajectory for $\nu = 3/2$ or $\mu = 1/4$.
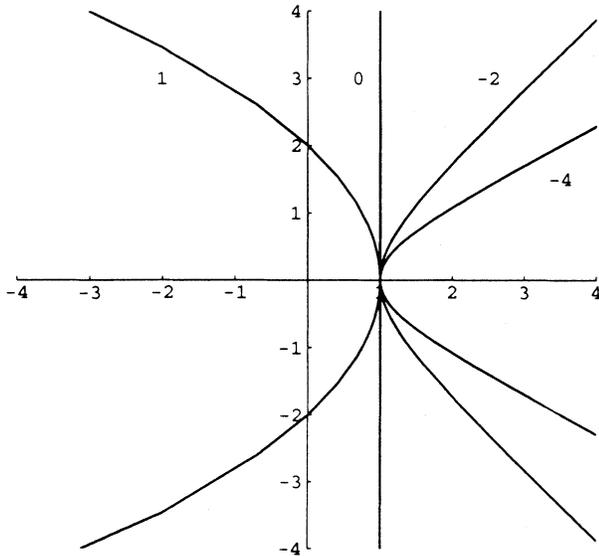
FIG. 12. From left to right, the trajectories for the cases $\nu = 1$ or $\mu = -1/2$; $\nu = 0$ or $\mu = -1$; $\nu = -2$ or $\mu = -2$; and $\nu = -4$ or $\mu = -3$. The curves are labeled by the numbers ν.

tential, with $\nu = \mu = -2$. The orbit is given by $\rho = [\cos 2\varphi]^{-1/2}$, so that

$$1 = \frac{r^2}{a^2} \cos 2\varphi = \frac{r^2}{a^2}(\cos^2 \varphi - \sin^2 \varphi) = \frac{x^2}{a^2} - \frac{y^2}{a^2} . \qquad (58)$$

Thus, the trajectory is a special hyperbolic orbit, whose minor and major axes are equal, $b^2 = a^2$. (In fact, every $\nu = -2$ solution, i.e., for arbitrary $E \neq 0$, also yields a hyperbolic orbit, but with $b \neq a$.) We show this orbit as the third drawing in Fig. 12. Now the angular width has decreased to $\pi/2$.

As the last case, we consider the orbit for $\nu = -4$ or $\mu = -3$. This orbit is shown in the last drawing of Fig. 12. The orbit subtends an angle of $\pi/3$, again as it should. One sees that as ν becomes more and more negative, the orbits will become narrower and narrower. This is just as in the bound case, where the petals became narrower and narrower as ν became more and more positive.

VII. DISCUSSION

A. Partner trajectories

The $\nu = 2$ or $\mu = 0$ circle ($r = a$) is the borderline between the bounded ($0 \leq r \leq a$) orbits for $\nu > 2$ or $\mu > 0$, and the unbounded trajectories ($a \leq r \leq \infty$) for $\nu < 2$ or $\mu < 0$. Moreover, because of the relation

$$\rho(-\mu, \varphi) = \frac{1}{\rho(\mu, \varphi)} , \qquad (59)$$

we can associate with every bounded orbit, which corresponds to $\mu > 0$ and lies on and inside the circle $r = a$

or $\rho = 1$, an unbounded counterpart, which belongs to negative μ and lies on and outside the circle. Since the opening angle of both of these trajectories is

$$\Phi_\nu = \frac{\pi}{|\mu|} , \qquad (60)$$

we call the members of these pairs partner trajectories.

The $\mu = 0$ or $\nu = 2$ circle $\rho = 1$ is the only trajectory which has itself as a partner. In our figures we have four examples of partner trajectories: (1) The first orbit for $\mu = 3$ or $\nu = 8$ in Fig. 4 is the partner trajectory to the $\mu = -3$ or $\nu = -4$ trajectory in Fig. 12. (2) The first orbit for $\mu = 2$ or $\nu = 6$ in Fig. 5 is the partner trajectory to the hyperbola $\mu = -2$ or $\nu = -2$ trajectory in Fig. 12. (3) The circle for $\mu = 1$ or $\nu = 4$ in Fig. 6 is the partner trajectory to the $\mu = -1$ or $\nu = 0$ straight line in Fig. 12. (4) The first double spiral for $\mu = 1/2$ or $\nu = 3$ shown in Fig. 7 is the partner trajectory to the trajectory $\mu = -1/2$ or $\nu = 1$ shown in Fig. 12.

B. Comments on the classical problem

It is well known that classical orbits precess for general central potentials. There are two exceptions, the Kepler and the isotropic harmonic oscillator potentials [4]. Further, these central potentials are known to have additional conserved quantities: the Runge-Lenz vector, **A**, in the Kepler problem and the quadrupole moment tensor, Q_{ij}, in the harmonic oscillator problem [25, 26]. These two examples show that there is a close connection between the absence of precession and the existence of dynamically conserved quantities.

On the other hand, it is also well known that for a specific energy to angular-momentum combination, general central potentials can have closed orbits. But these combinations have different unique values, depending upon the potential.

Therefore, it is interesting that the class of $E = 0$ solutions for the potentials (1) with $\nu > 2$ have a countable number of examples with well-defined, closed trajectories. They are all the potentials with rational values of ν. One of them, the case $\nu = 4$, has zero precession.

All the $E = 0$ with $\nu > 2$ solutions are bound and go through the origin. The $\nu < 2$ solutions are unbound, and go to infinity. (The $\nu = 2$ case is special, and does both.)

We have seen that, with the $\nu > 2$ singular potentials, the physical solutions differ from more familiar solutions in that, at the origin, we must paste together single-orbit solutions which have different phase shifts, φ_0^k, at $r = 0$. The discontinuity at the origin of the phase shifts, given by Eq. (29), is fundamental [27]. It is necessary because the bound orbits pass through the origin, where the potential is singular. This causes the second order time derivative of the position, i.e., the acceleration, to be infinite at $r = 0$ when $\nu \geq 2$:

$$\ddot{x}_i(t) = -\frac{\nu\gamma}{mr^{\nu+2}}x_i , \qquad i = 1, 2, 3 . \qquad (61)$$

Therefore, irrespective of what coordinate system we choose, at the origin we must still paste together dif-

ferent solutions of Newton's equation which depend on different initial conditions, as exhibited in Eq. (21).

As we have just observed, when crossing the center of singular potentials, a particle will have infinite momentum and kinetic energy. This leads to a violation of the virial theorem, even for these bound trajectories. Formally applying the virial theorem [28, 29] to power potentials leads to the following well-known equation:

$$\langle T \rangle = -\frac{\nu}{2} \langle V \rangle , \tag{62}$$

where $\langle T \rangle$ and $\langle V \rangle$ are the time averages of the kinetic and potential energies. The above equation leads to two famous relations: $\langle T \rangle = -\langle V \rangle/2$, for Kepler elliptical orbits ($E < 0$ and $\nu = 1$), and $\langle T \rangle = \langle V \rangle$ for the harmonic oscillator ($E > 0$ and $\nu = -2$).

From Eq. (62) and energy conservation, we have

$$E = T + V = \langle T \rangle + \langle V \rangle = \left(1 - \frac{2}{\nu}\right) \langle T \rangle . \tag{63}$$

Since $\langle T \rangle > 0$, Eq. (63) immediately shows that the virial theorem (62) is violated by all the $E = 0$ solutions of power potentials with $\nu \neq 2$. Such a violation of (62) is expected for infinite orbits, such as the parabolic orbit of the Kepler problem and all other $E = 0$, $\nu < 2$ orbits. What is of more interest is that the bound solutions, $\nu > 2$, also violate the theorem.

In summary, the classical $E = 0$ solutions for the power-law potentials exhibit a fascinating set of properties. In Ref. [12] we will show that this characteristic is also true for the quantum solutions.

APPENDIX A: ZERO ANGULAR-MOMENTUM SOLUTIONS

Here we discuss the simpler $E = L = 0$ solutions, where the effective potential $U(r)$ is equal to the potential

$V(r)$ itself. A particle moves radially, in a straight line, between zero and infinity, with no turning points at any finite radius, $r \neq 0$.

From the energy-conservation equation (12) one has that, for $E = L = 0$,

$$\frac{dr}{dt} = \pm \left(\frac{2\gamma}{m}\right)^{1/2} \frac{1}{r^{\nu/2}} \equiv v(t) . \tag{A1}$$

Unless $\nu = -2$ this is equivalent to

$$\frac{d(r)^{\nu/2+1}}{(\nu/2 + 1)dt} = \pm \left(\frac{2\gamma}{m}\right)^{1/2} , \tag{A2}$$

which has the solutions

$$r(t) = \left[r_0^{\frac{\nu+2}{2}} \pm \left(\frac{2\gamma}{m}\right)^{1/2} \left(\frac{\nu}{2} + 1\right) (t - t_0)\right]^{\frac{2}{\nu+2}} ,$$

$$\nu \neq -2, \tag{A3}$$

where $r_0 \equiv r(t_0)$.

The special case $\nu = -2$ yields the differential equation

$$\frac{dr}{dt} = \pm \left(\frac{2\gamma}{m}\right)^{1/2} r . \tag{A4}$$

The solutions are therefore

$$r(t) = r_0 \exp\left[\pm \left(\frac{2\gamma}{m}\right)^{1/2} (t - t_0)\right]$$

$$= r_0 \exp\left[\left(\frac{v_0}{r_0}\right) (t - t_0)\right] . \tag{A5}$$

(The exponential solution (A5) follows from the general solution (A3), by using $\lim_{\epsilon \to 0}(1 + \epsilon x)^{1/\epsilon} = \exp[x]$.)

For this $L = 0$ case, the complete journey from the origin to infinity takes an infinite amount of time for *all* indices $-\infty < \nu < \infty$.

[1] E. Schrödinger, Naturwissenschaften **14**, 664 (1926), translated into English in E. Schrödinger, *Collected Papers on Wave Mechanics*, 2nd ed. (Blackie & Son, London, 1928), pp. 41–44.

[2] F. Steiner, Physica B **151**, 323 (1988), describes Schrödinger's discovery of the coherent states [1], and the interactions among he, Lorentz, Heisenberg, and others.

[3] T. T. Taylor, *Mechanics: Classical and Quantum* (Pergamon, Oxford, 1976).

[4] M. J. Bertrand, CR Acad. Sci. (Paris) **77**, 849 (1875).

[5] P. M. Morse, Phys. Rev. **34**, 57 (1929).

[6] N. Rosen and P. M. Morse, Phys. Rev. **42**, 210 (1932).

[7] G. Pöschl and E. Teller, Zeit. Phys. **83**, 143 (1933).

[8] W. C. DeMarcus, Am. J. Phys. **46**, 733 (1976).

[9] M. M. Nieto and L. M. Simmons, Jr., Phys. Rev. D **20**, 1342 (1979).

[10] M. M. Nieto and L. M. Simmons, Jr., Phys. Rev. D **20**, 1332 (1979).

[11] C. Zhu and J. R. Klauder, Am. J. Phys. **61**, 605 (1993).

[12] J. Daboul and M. M. Nieto (unpublished). Also see J. Daboul and M. M. Nieto, Phys. Lett. A **190**, 357 (1994).

[13] H. Goldstein, *Classical Mechanics*, 2nd ed. (Addison-Wesley, New York, 1980).

[14] Equation (3.36), p. 87, in Ref. [13].

[15] M. R. Spiegel, *Schaum's Outline of Theory and Problems on Theoretical Mechanics* (McGraw-Hill, New York, 1967).

[16] Equation (11), p. 117, in Ref. [15].

[17] Figure 3-12, p. 87, in Ref. [13].

[18] I. S. Gradshteyn and I. M Ryzhik, *Table of Integrals, Series, and Products* (Academic Press, New York, 1965), integral 3.621.5.

[19] *Higher Transcendental Functions, Vol. I*, edited by A. Erdélyi (McGraw-Hill, New York, 1953), p. 47, Eq. (5).

[20] Problem 5.60, p. 138, in Ref. [15].

[21] Section 5.15, p. 127, in Ref. [15].

[22] J. B. Marion and S. T. Thornton, *Classical Dynamics*, 3rd ed. (Harcourt Brace Jovanovich, New York, 1988), p.

287.

[23] L. D. Landau and E. M. Lifshitz, *Mechanics*, 3rd ed. (Pergamon Press, New York, 1976).

[24] Chapter IV, Art. 15, problem 2, p. 40 in Ref. [23].

[25] Section 9-7, p. 420, in Ref. [13].

[26] L. I. Schiff, *Quantum Mechanics*, 3rd ed. (McGraw-Hill, New York, 1968), Chap. 7, Sec. 30, p. 234.

[27] The discontinuity at the origin of the azimuthal angle, φ, by π, is only a technical problem associated with the nature of polar coordinates. It disappears in Cartesian coordinates because both $x(t)$ and $y(t)$ are continuous functions of time.

[28] Section 3-4, p. 82 in Ref. [13].

[29] Chapter II, Art. 10, p. 23 in Ref. [23].